Effects of water-absorption and thermal drift on a polymeric photonic crystal slab sensor

Sørensen, Kristian Tølbøl; Ingvorsen, Charlotte Bonde; Nielsen, Line Hagner; Kristensen, Anders

Published in:
Optics Express

Link to article, DOI:
10.1364/OE.26.005416

Publication date:
2018

Document Version
Publisher's PDF, also known as Version of record

Research Article | Vol. 26, No. 5 | 5 Mar 2018 | OPTICS EXPRESS 5416
Optics EXPRESS

Effects of water-absorption and thermal drift on a polymeric photonic crystal slab sensor

KRISTIAN TØLBØL SØRENSEN,[1] CHARLOTTE BONDE INGVORSEN,[1] LINE HAGNER NIELSEN,[1] AND ANDERS KRISTENSEN[1,*]

[1]*DTU Nanotech, Technical University of Denmark, Ørsteds Plads building 345C, 2800 Kgs. Lyngby, Denmark.*
[*]*anders.kristensen@nanotech.dtu.dk*

Abstract: A photonic crystal slab (PCS) sensor is a universal refractive index sensor with possibilities and performance very similar to surface plasmon resonance (SPR), which represents the gold standard of biosensing. Cheap PCS sensors can be made vacuum-free entirely out of polymers, but come with additional challenges, besides those relating to temperature-variations, which must be considered in any refractive index based method: The polymeric waveguide core was found to swell by ~0.3% as water absorbed into the waveguide core over ~1.5 h. This was investigated by monitoring the wavelength of resonant reflection during absorption, by monitoring the release of water using ellipsometry, and by rigorous coupled-wave analysis (RCWA). The approach presented here enables monitoring of water uptake and thermal fluctuations, for drift-free, high-performance operation of a polymeric PCS sensor.

OCIS codes: (240.0240) Optics at surfaces; (050.5298) Photonic crystals; (220.4241) Nanostructure fabrication; (280.4788) Optical sensing and sensors; (310.2785) Guided wave applications.

References and links

1. G. G. Nenninger, M. Piliarik, and J. Homola, "Data analysis for optical sensors based on spectroscopy of surface plasmons," Meas. Sci. Technol. **13**, 2038–2046 (2002).
2. I. D. Block, L. L. Chan, and B. T. Cunningham, "Large-area submicron replica molding of porous low-k dielectric films and application to photonic crystal biosensor fabrication," Microelectron. Eng. **84**, 603–608 (2007).
3. M. Piliarik and J. Homola, "Surface plasmon resonance (SPR) sensors: approaching their limits?" Opt. Express **17**, 16505 (2009).
4. R. Magnusson and S. S. Wang, "New principle for optical filters," Appl. Phys. Lett. **61**, 1022–1024 (1992).
5. B. T. Cunningham, "Label-Free Assays on the BIND System," J. Biomol. Screen. **9**, 481–490 (2004).
6. R. Magnusson and M. Shokooh-Saremi, "Physical basis for wideband resonant reflectors," Opt. Express **16**, 3456–3462 (2008).
7. K. Bougot-Robin, S. Li, Y. Zhang, I.-M. Hsing, H. Benisty, and W. Wen, ""Peak tracking chip" for label-free optical detection of bio-molecular interaction and bulk sensing," The Analyst **137**, 4785–4794 (2012).
8. P. G. Hermannsson, K. T. Sørensen, C. Vannahme, C. L. Smith, J. J. Klein, M.-M. Russew, G. Grützner, and A. Kristensen, "All-polymer photonic crystal slab sensor," Opt. Express **23**, 16529–16539 (2015).
9. Y. Nazirizadeh, V. Behrends, A. Prósz, N. Orgovan, R. Horvath, A. M. Ferrie, Y. Fang, C. Selhuber-Unkel, and M. Gerken, "Intensity interrogation near cutoff resonance for label-free cellular profiling," Sci. Reports **6**, 24685 (2016).
10. Y. C. Lin, W. H. Hsieh, L. K. Chau, and G. E. Chang, "Intensity-detection-based guided-mode-resonance optofluidic biosensing system for rapid, low-cost, label-free detection," Sensors Actuators, B: Chem. **250**, 659–666 (2017).
11. D. Gallegos, K. D. Long, H. Yu, P. P. Clark, Y. Lin, S. George, P. Nath, and B. T. Cunningham, "Label-free biodetection using a smartphone," Lab on a Chip **13**, 2124 (2013).
12. B. Cunningham, B. Lin, J. Qiu, P. Li, J. Pepper, and B. Hugh, "A plastic colorimetric resonant optical biosensor for multiparallel detection of label-free biochemical interactions," Sensors Actuators, B: Chem. **85**, 219–226 (2002).
13. D. Threm, Y. Nazirizadeh, and M. Gerken, "Photonic crystal biosensors towards on-chip integration," J. Biophotonics **5**, 601–616 (2012).
14. M. Daimon and A. Masumura, "Measurement of the refractive index of distilled water from the near-infrared region to the ultraviolet region," Appl. Opt. **46**, 3811 (2007).
15. M. F. Pineda, L. L.-Y. Chan, T. Kuhlenschmidt, C. J. Choi, M. Kuhlenschmidt, and B. T. Cunningham, "Rapid Specific and Label-Free Detection of Porcine Rotavirus Using Photonic Crystal Biosensors," IEEE Sensors J. **9**, 470–477 (2009).

#314922 https://doi.org/10.1364/OE.26.005416
Journal © 2018 Received 12 Dec 2017; revised 4 Feb 2018; accepted 15 Feb 2018; published 22 Feb 2018

Optics EXPRESS

16. R. Magnusson, D. Wawro, S. Zimmerman, and Y. Ding, "Resonant photonic biosensors with polarization-based multiparametric discrimination in each channel," Sensors. **11**, 1476–1488 (2011).
17. P. G. Hermannsson, C. Vannahme, C. L. C. Smith, K. T. Sørensen, and A. Kristensen, "Refractive index dispersion sensing using an array of photonic crystal resonant reflectors," Appl. Phys. Lett. **107,** 061101 (2015).
18. A. Yariv and P. Yeh, *Photonics: Optical electronics in modern communications* (Oxford University Press, 2007), 6th ed.

1. Introduction

Surface plasmon resonance (SPR) has become a gold standard [1, 2] for label-free biomolecular investigations with excellent detection limits on the order of 10^{-6} RIU [3]. However, the technique places high demands on both chips and readout instrumentation, making the technology expensive to both acquire and employ. An alternative class of optical sensor exists, known as a guided mode resonance filter [4, 5], leaky-mode reflector [6], resonant waveguide grating [7], or, as it will referred to here, a photonic crystal slab (PCS) sensor [8]. Compared to SPR, this sensor can be read out using much simpler instrumentation, such as an LED and a photodiode [9, 10] or even a smartphone [11]. Roll-to-roll high-throughput fabrication was demonstrated at an early stage [12], and microwell plates with PCS sensors on the bottom are commercially available, e.g. Corning Epic Microplates (Tewksbury, MA, USA). However, the price-tag may pose a barrier to many potential applications.

For the lowest possible cost price of consumables, it is desirable to have the sensors made entirely out of polymers. The feasibility of this has already been documented [8], yet for the cheap polymeric optical sensors to be competitive with those produced using expensive vacuum-based methods, the device operation must be highly optimimzed. In this work, we outline best practices for achieving high performance using a polymeric PCS sensor.

Refractive index sensors are universal in the sense that almost any change to a fluid will change its refractive index, making the sensor capable of monitoring practically any change in the fluid. This versatility comes at the cost of increased demands for variable control, as refractive index itself is sensitive to, e.g., thermal fluctuations. PCS sensors tend to amplify such fluctuations, as the permittivities of the materials constituting the sensor are also affected by temperature. Obviously, the issue may be alleviated by thermal control [1, 13], however, a 0.1 °C increase in temperature still reduces the refractive index of water by $\Delta n_D = 1 \cdot 10^{-5}$ RIU [14], which may additionally be amplified several times by the PCS. Furthermore, in order to monitor transient effects, thermal compensation is desirable.

In order to cancel out thermal contributions, a common approach is to have neighboring sensors serve as references [5, 15]. Alternatively, transverse electric (TE)- and transverse magnetic (TM)-mode resonances can be monitored simultaneously [16], uniquely enabling referencing at the exact same physical location. As the mode confinement differs between the resonances of the two light polarizations, one resonance predominantly responds to events at the surface, whereas the other is more sensitive to the bulk. In this work, we produce a reference region on a part of the sensor surface, such that both sample and reference regions may be read out simultaneously and in close proximity, as illustrated in fig. 1.

2. Method

A polymeric PCS sensor was fabricated based on previous work [8]. A 2 mm thick slab of poly(methyl methacrylate) (PMMA) was laser-cut to a diameter of 100 mm and plasma-treated (Pico Plasma Asher, Diener Electronic, Germany) for hydrophilicity. A droplet of low-refractive index polymer Efiron AC409-AP (Luvantix, Korea, n_D=1.40), diluted to 85% w/w in 2-butanone (Sigma-Aldrich, MO, USA), was then sandwiched between the PMMA substrate and a silicon stamp. The stamp had been defined by electron-beam lithography to contain 4×4 areas of 2 mm $\times$ 2 mm, each containing a linear grating of period $\Lambda = 368$ nm and depth $d = 100$ nm.

Optics EXPRESS

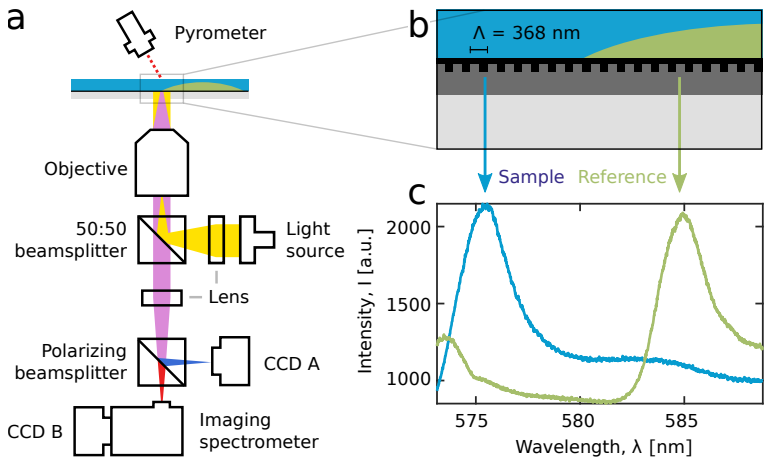

Fig. 1. Experimental setup and operating principle of the PCS sensor, using a) an optical setup which ensures collimated, normal incidence illumination of the b) sensor, illustrated here in cross-section (not to scale). A reference material partially covers the sensor, increasing the c) resonance wavelength relative to the sample.

After curing by a 1000 W UV flood exposure (Oriel Flood Exposure Source, Newport Corp., CA, USA), the substrate was separated from the stamp and baked at 90 °C for 3 min. The high-refractive index dielectric waveguide core was produced either using ion beam sputter deposition (Ionfab 300, Oxford Instruments, GB) of 80 nm titania (TiO_2, n_D=2.61), or by polymer spincoating (Süss MicroTec, Germany) for a genuinely polymeric sensor. In that case, a high-refractive index polymer HI01XP (micro resist technologies GmbH, Germany, n_D=1.59), diluted to 15% w/w in ma-T 1050 (micro resist technologies) was spincoated at 3,000 rpm for 1 min. The layer was then UV flood exposed in oxygen-free atmosphere for 5 min.

The thus finished PCS sensor subsequently had small droplets of Efiron manually deposited, such that they covered a part of each sensor. Following oxygen-free UV curing, the resulting reference regions typically had a diameter 400–1000 μm and a height of 10–50 μm as ascertained by profilometry (Dektak 8, Veeco Instruments, NY, USA, data not shown). This part of the fabrication process is suitable for patterning, e.g., via photolithography, but the full process would need to be compatible with the chemical and physical stability of all polymers involved. For characterizing the evolution of thin-film thickness and refractive index over time, variable angle spectroscopic ellipsometry (J.A. Woollam, NE, USA) was used.

The laboratory setup is described in [17], and illustrated in fig. 1. Where nothing else is stated, components were purchased from Thorlabs (NJ, USA). Briefly, white light from a bright and spectrally flat light source (EQ-99X LDLS, Energetiq, MA, USA) was output through a fiber collimator onto an adjustable mirror, shining through a focusing lens onto a 50-50 beamsplitter, through a 4× objective, ensuring collimated input light interacting with the sensor at nominally normal incidence. The sensor wafer was mounted on a motorized stage. Reflected light was transmitted through the objective and beamsplitter, encountering a mirror and tube lens before reaching a polarizing beamsplitter. TM-polarized light was collected by the imaging CCD A, whereas TE-polarized light, containining a resonance peak, was received by CCD B of an imaging spectrometer (Acton SP2750, Princeton Instruments, NJ, USA). A pyrometer (CSlaser LT hs CF1, Optris GmbH, Germany) was mounted on the stage and focused on the water droplet in cases where complementary temperature monitoring was used. To avoid evaporation during long time series, an air-tight lid was placed on top of the wetted sensor.

The imaging spectrometer was operated at an effective integration time of 0.1–30 s, depending

Optics EXPRESS

on the desired temporal resolution. Each spectral image was recorded using LightField 6.2 (Princeton Instruments) and contained 100 spectra, providing a one-dimensional spatial resolution of 5 μm. Each spectrum was resolved into 1340 pixels with a spectral resolution of 12 pm. Time series of up to 1000 frames were imported into MATLAB 2016b (The MathWorks Inc., MA, USA) using a custom function and organized into a 3D matrix, thus containing up to $1.34{\cdot}10^8$ intensity values of 32 bit depth. The matrix dimensionality was first reduced to 2D by calculating the centroid resonance wavelength of each spectrum after a 50% thresholding, and then to 1D by binning the sample- and reference regions.

Rigorous coupled-wave analysis (RCWA) simulations were carried out using the Grating Diffraction Calculator (KJ Innovation, CA, USA) package implemented in MATLAB. The model was set up with the refractive index dispersion of Efiron and HI01XP as substrate and waveguide core layers, respectively. The grating had a period of 368 nm and a depth of 100 nm. The core thickness was 183 nm, in accordance with ellipsometer measurements, and the angle of incidence was 0°. A custom algorithm for adaptive resolution refinement was used to locate and adequately resolve all spectral features.

3. Results and discussion

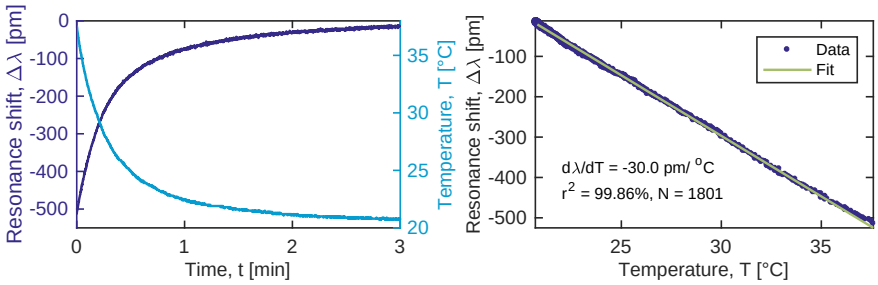

Fig. 2. a) A deliberate temperature perturbation reveals b) the thermo-optic coefficient of the sensor in water, by correlating the resonance wavelength shift with temperature as measured by a pyrometer.

The amplified temperature sensitivity due to thermally induced refractive index changes in the sensor stack, was investigated by adding a droplet of heated water to a thermally equilibrated volume of water sitting on a titania-type sensor. The result is shown in fig. 2. The temperature was measured using a pyrometer simultaneously with resonance shift monitoring. The refractive index sensitivity of these sensors was determined by monitoring the resonance shift in response to sucrose solutions of known refractive index, and found to be $d\lambda/dn = 90$ nm/RIU. The effective thermo-optic coefficient of the sensor in water was determined to be $dn/dT = 3.3 \cdot 10^{-4}$ RIU/°C, an amplification of 3.3× compared to the thermo-optic coefficient of water itself [14], potentially making temperature control insufficient and exacerbating the need for thermal referencing.

For a PCS sensor, the resonance shift measured in a sample S can be considered $\Delta\lambda_S = \sum_i \Delta\lambda_i$, where $\Delta\lambda_i$ are the individual contributions making up the resonance shift. Assuming the sensor itself to be stable over time, and that the analyte does not adhere to the sensor surface, the observed resonance shift is expected to have only two contributions, namely changes in analyte concentration Δc and temperature ΔT. Thus, $\Delta\lambda_S = \Delta\lambda_{\Delta c} + \Delta\lambda_{\Delta T}$. Although the $\Delta\lambda_{\Delta T}$ term is straightforwardly determined using a pyrometer as described, this would be unsuitable for the many promising applications involving microfluidics [13], while increasing cost and complexity of the necessary instrumentation. Alternatively, the temperature-contribution may be isolated by making a sensor region insensitive to the liquid composition, while retaining its sensitivity to temperature fluctuations. In practice, this was achieved by shielding the reference region

Optics EXPRESS

R with a polymer layer of thickness greater than the mode overlap. The electric field of the polymeric TE-mode sensors used here is described by $E(x, y, z, t) \propto E_m(x) = C\exp(-qx)$ in the superstrate [18], where x is the distance from the sensor surface and $q = \sqrt{\beta^2 - n_1^2 k_0^2}$ [17]. The propagation constant β must satisfy the phase matching condition $\beta = 2\pi/\Lambda$ [8]. For this system, the penetration depth, i.e., the distance $\hat{e}$ where the electric field has decayed to $E_m(\hat{e})/E_m(0) = 1/e$, is $\hat{e} = 138$ nm in water, meaning that 99.999% of the sensor sensitivity is found within the first 1.3 μm from the surface. Ensuring that the reference polymer is thicker than this, but still very thin in order to minimize lag, thermal fluctuations will transfer to the sensor through the polymer, enabling drift compensation. Changes in analyte concentration will then not affect the reference region.

The part of a resonance shift originating from the temperature contribution is expressed as $\Delta\lambda_{\Delta T} = \Delta\lambda_R \cdot C$, where $\Delta\lambda_R$ is the resonance shift measured in the reference region, and C is an empirical constant, that takes into account the thermo-optic coefficients dn/dT of the sample, reference polymer, and each component of the sensor stack. Then, assuming that the bulk concentration change is $\Delta c = 0$, the resonance shift measured in the sample correlates with the resonance shift in the reference region as $\Delta\lambda_S = 0 + \Delta\lambda_R \cdot C$. Once C has been determined, the resonance shift owing solely to concentration changes is

$$\Delta\lambda_{\Delta c} = \Delta\lambda_S - C \cdot \Delta\lambda_R \tag{1}$$

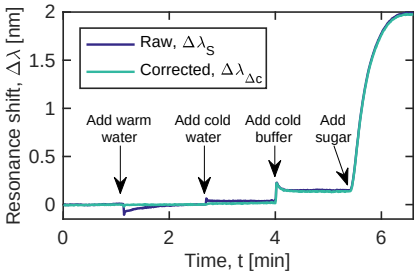

Fig. 3. Temperature perturbations are effectively cancelled by thermal compensation, ensuring a stable and drift-free baseline. With thermal effects accounted for, the time for full mixing of the buffer becomes clearly visible at $t = 4$ min.

With effective temperature compensation, a flat baseline can be achieved even in the presence of drift and sample perturbations, as shown in fig. 3. A steady baseline is disturbed by the addition of warm and cold water at $t = 1.1$ min and $t = 2.6$ min, respectively. The only difference here would be a slight temperature variation, which is effectively canceled by the thermal compensation method, maintaining a stable baseline. Then, at $t = 4.0$ min, buffer is added. This time, a perturbation is caused by both the mixing of buffer salts with the existing sample, as well as a slight temperature fluctuation. Due to the independence from thermal contributions afforded by the method, sample mixing time is decoupled from the thermal equilibration process, and full mixing is observed to take ~ 15 s.

So far, we have only discussed the situation where the only two contributions to the measured resonance shift is assumed to be concentration and temperature changes. However, additional contributions can be relevant to certain applications, e.g., for biosensors, a contribution from biorecognition events would be the main parameter of interest. When additional contributions are present, $\Delta\lambda_{\Delta c=0} = \Delta\lambda_S - C \cdot \Delta\lambda_R \neq 0$, and hence the model can also be used to check for additional, perhaps unexpected contributions.

Figure 4 illustrates such a situation, where at $t = 0$, the dry sensor is exposed to water and enclosed under a lid. Initially, both resonance regions shift together, but soon, only the sample

Optics EXPRESS

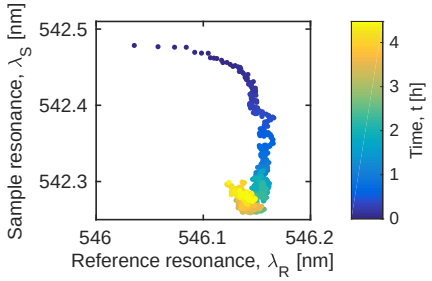

Fig. 4. Resonance wavelength of the sample region (λ_S) versus the reference region (λ_R) over time. Following approx. 5 minutes of temperature equilibration, the blue-shifting of the sample resonance over the first ~ 1.5 h may be due to water absorption into the exposed waveguide core. The shielded reference region is relatively stable during the period.

resonane has an appreciable shift. As the water sample is unperturbed, this can neither be due to evaporation, other changes in bulk concentration, non-specific analyte binding, nor temperature drift. Rather, it is hypothesized that water slowly absorbs into the polymeric waveguide core layer. A some-hours long equilibration time is consistently observed when wetting polymeric PCS sensors, however, the magnitude and duration varies, possibly due to varying environmental conditions such as air humidity prior to wetting. In case water uptake happens by displacement or dissolution of microscopic air pockets, the waveguide core refractive index should increase. If it happens through swelling of the polymer, the refractive index should decrease.

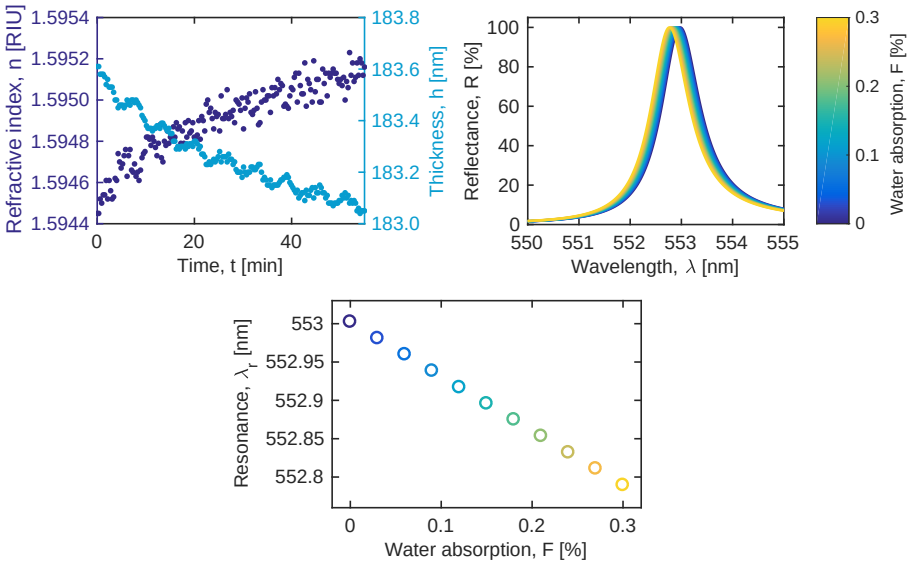

Fig. 5. Water degassing investigated by a) ellipsometer, indicating concomitant core layer shrinking and refractive index increase, and by b) RCWA in response to the changes measured by ellipsometry, indicating c) 215 pm of simulated resonance shift. The result is consistent with the direct sensor readout data.

The observed blue-shifting of the sample resonance wavelength by hundreds of picometers is consistent with a reduction of the waveguide core refractive index, i.e., swelling of the polymer matrix. In order to investigate this, an ellipsometer was used to monitor the outgassing of a sensor wafer which had been submerged in water overnight. The results are shown in fig. 5(a), and

Optics EXPRESS

indicate an increase in waveguide core refractive index and a concomitant decrease in thickness, in agreement with the hypothesized swelling from water absorption. When F is the fraction of the core volume comprised of water, the core refractive index n_{core} at 589 nm is assumed to be described by

$$n_{\text{core}} = n_w F + n_p(1 - F) \tag{2}$$

where n_w=1.33 and n_p=1.59 are the refractive indices at 589 nm of water and core-polymer, respectively. Thus, the measured change in refractive index corresponds to a water content of $F = 0.3\%$. It is noted that the change in thickness over this period is also $\sim 0.3\%$.

The effect of water absorption into the waveguide core layer was furthermore investigated by RCWA, as shown in fig. 5(b). A shift of 215 pm is observed when the waveguide core thickness increases by up to 0.3%, and its refractive index decreases similarly. This shift is in agreement with the experimental observations. Thus, for high-performance operation of a polymeric PCS sensor, in practice, it must be primed for hours prior to use, and thermal contributions must be accurately isolated.

4. Conclusion and outlook

In summary, we have shown that by fabricating a reference region of known refractive index, thermal drift can be fully compensated, in practice improving the performance of polymeric PCS sensors. By reliable decoupling of thermal effects from the sensor readout, it was established by three complementary techniques that the polymeric PCS sensors absorb $\sim 0.3\%$ water over several hours, after which they remaining stable. Thus, devices should always be primed before use. Polymeric PCS sensors can be produced at a much lower price than conventional PCS sensors, although the requirement for constant wetting makes them more suitable for microfluidic integration than as free-standing sensors.

Funding

Danish Council for Strategic Research, (DSF, Grant No. 10-092322); Danish National Research Foundation (DNRF122); Villum Fonden for Intelligent Drug Delivery and Sensing Using Microcontainers and Nanomechanics (IDUN) (Grant No. 9301); Danish Research Council for Technology and Production (FTP) Project (DFF 4004-00120B).